

A Study on the Morphology, Mechanical, and Electrical Performance of Polyaniline-modified Wood - A Semiconducting Composite Material

Beatriz I. Hassel,^{a,*} Stacy Trey,^{b,d} Simon Leijonmarck,^{b,e} and Mats Johansson^{b,c}

This study investigated the morphology, electrochemical modification with respect to the wood fiber direction, and mechanical properties of wood modified by *in situ* polymerization with polyaniline (PANI). This polymerization formed a composite material with applications as an anti-static, electromagnetic, anti-corrosion, and heavy metal purifying materials. The polymer was found throughout the entire structure of the wood and was quantified within the wood cell wall and middle lamella by SEM-EDX. The presence of PANI affected the conductivity of the composite specimens, which was found to be higher in the fiber direction, indicating a more intact percolation pathway of connected PANI particles in this direction. The PANI modification resulted in a small reduction of the storage modulus, the maximum strength, and the ductility of the wood, with decreases in the properties of specimens conditioned in an environment above 66% relative humidity. The *in situ*-polymerized PANI strongly interacted with the lignin component of the veneers, according to the decrease in the lignin glass transition temperature (T_g) noted in DMA studies.

Keywords: Smart materials; Electrical properties; Mechanical properties; Electron microscopy

Contact information: a: Department of Engineering Sciences, Division of Applied Mechanics, Uppsala University, Ångströmlab, Lägerhyddsvägen 1, 75237 Uppsala, Sweden; b: Wallenberg Wood Science Centre (WWSC), KTH Royal Institute of Technology, Teknikringen 56-58, SE-100 44 Stockholm, Sweden; c: Department of Fibre and Polymer Technology, KTH Royal Institute of Technology, SE-10044 Stockholm, Sweden; d: SP Technical Research Institute of Sweden, Department of Wood Technology, Box 5609, Drottning Kristinas väg 67, SE-114 86, Stockholm, Sweden; e: Department of Chemical Engineering, KTH Royal Institute of Technology, SE-10044 Stockholm, Sweden;
Corresponding author: Tel.: +4618-471 2790. E-mail address: Ivon.Hassel@angstrom.uu.se

INTRODUCTION

Interest in intrinsically conductive materials (ICPs) has steadily increased over the past few decades. The most prominent recognition in the area was the 2000 Nobel Prize in chemistry for the development of conductive polymers, awarded to Heeger, MacDiarmid, and Shirakawa (Heeger 2001; Rimbú *et al.* 2006). Among the numerous conducting polymers, including polypyrrole, polyacetylene, and polythiophene, polyaniline is most often studied because of its low cost, easy and controllable synthesis, environmental stability, high electrical conductivity, and ease of blending with other polymers (Madani *et al.* 2010). Polyaniline is an insulator unless it is oxidized with a protic acid. The doping or protonation of the polymer can be tuned to adjust its degree of conductivity (Wolszczak and Abdel-Hamid 1995). These characteristics give polyaniline potential within many different applications, including electronic devices, batteries, solar cells, anti-static materials, electric heaters, and even the filtration of heavy metals (Park *et al.* 2004; Ansari 2006; Jafarzadeh *et al.* 2013; Saini and Arora 2013). Because of the poor mechanical

properties of ICPs and the difficulties associated with dissolving or melting them, they have often been combined with traditional thermoplastics, such as polyethylene terephthalate and polyethylene, to obtain a suitable balance between conductivity and mechanical performance (Qaiser *et al.* 2009). However, there is still need for improvement in both the electrical and mechanical performance of this class of material.

In recent research, forest products such as cellulose and other natural fibers have been coated with polyaniline (Olson *et al.* 2010, Razak *et al.* 2013). This allows for flexible composites; however they have the disadvantage of very low mechanical strength when wet and usually require a separate scaffold for many of the envisioned applications. Wood veneers have been made semiconductive by impregnating and growing polyaniline particles *in situ* into the wood structure (Trey *et al.* 2012; Treu *et al.* 2014). The veneer acts as a lightweight structural template, allowing for the formation of a composite material with tunable conductivity and significant mechanical strength. Polyaniline has the advantage over other conductive fillers like carbon nanotubes and graphene in that it can be absorbed by wood in the monomer state and form particles *in-situ*. This allows for ideal dispersion and full use of the light and strong wood structure as a template. Polyaniline was chosen from the array of conductive polymers because it is one of the few that begins as an aqueous monomer solution. The wood structure is able to absorb the polyaniline and subsequently swells to indicate the solution is taken up in the cell walls and allow particle deposition throughout. This will allow for maximum surface area contact and may be an ideal scaffold for one of the newly researched areas of protonated polyaniline used for the removal of aqueous heavy metals such as Cr (Vi) for applications including the purification of drinking water (Wang *et al.* 2014)

Wood is a three-dimensional, anisotropic, cellular solid made up of highly elongated, hollow cells called tracheids (Heinz and Leibert 2001). On the millimeter scale, it is composed of hexagonally-shaped cell walls enclosing empty pore spaces, or lumen. The mechanical properties of wood depend primarily on the properties of the cell wall, its relative density, and the shape of the walls themselves.

On the micrometer scale, wood is a fiber-reinforced composite. The cell walls are made of fibers of crystalline cellulose embedded within a matrix of amorphous hemicellulose and lignin, the latter hydrophobic. Each wood cell, glued together with a thin layer composed mainly of lignin, is made up of a primary wall and a secondary wall, each with different chemistries and structures. Although cellulose, hemicellulose, and lignin are each present in all of the layers of the cell wall, they vary in amount in each cell wall region. Overall, lignin is the dominant component, but it decreases in quantity towards the lumen.

The cellulose crystal lattice is held together by intermolecular and dipolar interactions, primarily in the form of hydrogen bonds. Because of the strength of these cumulative, secondary interactions, the chains are insoluble in water and most chemicals. This provides a 3-D matrix that can be used to reinforce materials that cannot stand on their own.

It is becoming increasingly important to develop value-added forest-based products due to the declining use of forest products in traditional markets (*e.g.*, newspapers). Using resources with better overall sustainability is also becoming more favorable (Mohani *et al.* 2002). Wood is therefore an ideal candidate for the substitution of traditional, petroleum-based, plastic matrices in many applications.

Although previously studied by other authors, there is still little knowledge of how the water-soluble monomer aniline interacts with wood and polymerizes to form PANI inside the wood structure. It is also largely unknown how this affects the properties of the material. This study investigates the morphology of wood veneers modified with

polyaniline and the effect of the modification on the moisture sensitivity, mechanical properties, and since wood is an anisotropic material, conductive properties were measured both across the fibers of wood (against the grain) and in parallel (with the grain).

EXPERIMENTAL

Materials

Aniline (greater than 99.5% purity), phosphoric acid (85 wt. % in H₂O, 99.9% trace metal basis), and peroxydisulfate (greater than 98.0%) were used as received from Sigma Aldrich (Schnellendorf, Germany). Carolina Southern yellow pine (*Pinus palustris*) veneers were cut according to the half-round slicing method and were supplied by Capital Crispin Veneer (London). The annual rings had an average periodicity of 7 to 8 mm. All chemicals were purchased from Sigma Aldrich unless otherwise noted.

Methods

Impregnation/polymerization procedure

The veneers were cut to dimensions of 0.6 mm × 50.0 mm × 50.0 mm in sets of 5 and were vacuum-pressure impregnated for 24 h at 10 bar in an inert atmosphere. During the first hour, the solutions were kept at 0 °C. They were kept at room temperature for the remainder of the 24-h impregnation. The solution used consisted of aniline in water with a concentration of 0.20 M phosphoric acid (PA), a dopant-to-aniline molar ratio of 1, and a peroxydisulfate-to-aniline ratio of 1.25. These reactant ratios have been found to result in the emeraldine salt form of polyaniline, with 50% of the emeraldine base protonated or oxidized (Fig. 1) (Huang *et al.* 1986). The samples were then dried in a vacuum oven at 50 °C for 48 h. Polyaniline particles (PANI) formed in the solution containing the wood blocks, and after 48 h, the modified blocks were removed.

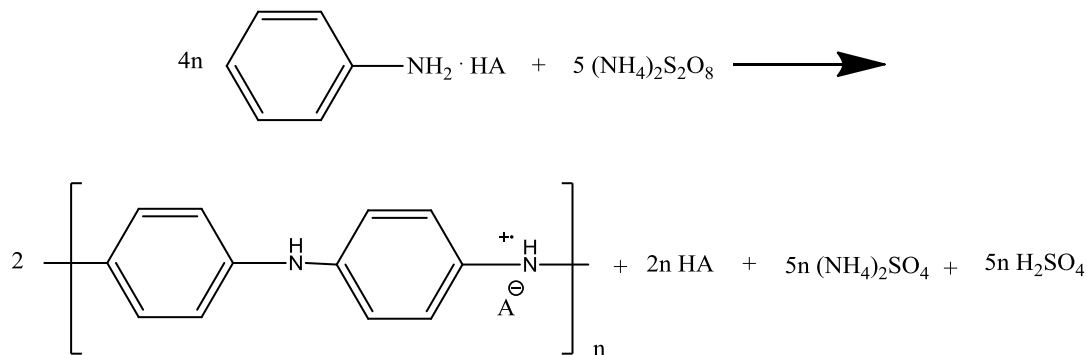


Fig. 1. Mechanism of reaction forming 50% oxidized polyaniline

Sampling selection of the modified veneers

Once impregnated, the veneers were conditioned to three different relative humidities (RH). Each micro-environment was created inside a desiccator containing a solution of deionized water and the appropriate salt with a hygrometer. Silica gel was used to create a 0% RH environment, while sodium nitrite (NaNO₂) created a 66% and copper sulfate pentahydrate (CuSO₄•5H₂O) created a 98% RH environment.

Areas of earlywood (EW) and latewood (LW) were visually selected from larger pieces of veneer. Specimens for tensile testing, conductivity testing, and dynamic mechanical analysis (DMA) were cut with a razor blade. Samples were laser-cut for SEM

imaging in order to prevent any bending or distorting of the wood cells.

Both PA-treated and untreated EW and LW samples were conditioned to 0, 66, and 98% RH, for a total of 12 samples.

The density of the samples was measured for each RH condition. To calculate the moisture content (MC), Eq. (1) was used,

$$(\%)MC = \left(\frac{W_w - W_d}{W_d} \right) * 100 \quad (1)$$

where W_w is the initial weight (in the conditioned, wet state) and W_d is the final, dry weight of each sample (oven-dried at 105 °C to a constant mass). Once conditioned, the density and moisture content (MC) of the veneers were calculated.

Preparation of specimens by excimer laser

Veneers of dimensions 0.5 mm x 10 mm x 70 mm were ablated transverse to the fiber direction to give a cross-section of dimensions 0.5 mm x 10 mm, using a PM-886 pulsing UV (KrF) excimer laser (GSI Lumonics; Northville, MI, USA) of wavelength 248 nm. A gas blend of 0.07% fluorine, 1.3% krypton, and 98% neon was used. The pulse energy was 300 mJ, at 30 to 35 kV, with a pulse repetition frequency of 5 Hz.

Tensile tests

Eight replicate samples of each type, each with dimensions of 0.5 mm x 10 mm x 70 mm, were cut with the longest side along the fiber direction. Sandpaper with dimensions of 10 mm x 0.5 mm was glued to the ends of each sample on both sides, preventing slippage from the grips of the testing machine. A pressure of 0.77 MPa was applied by the grips. A black speckle pattern was applied to one of the surfaces of each specimen to create a recognizable, greyscale pattern. Tensile load was applied with an Instron (Danderyd, SE) universal testing machine 5567, equipped with a 2-kN load cell, at a cross-head speed of 0.5 mm/min until failure of the samples occurred.

Strain measurements were made using a non-contact technique with a digital image correlation system (DIC), Vic-2D (Correlated Solutions; Columbia, SC, USA). A CCD camera with a single-lens Nikon 24-85mm f/2.8-4 (AF-D NIKKOR) was used. The post-processing of the pictures was done with commercially available DIC software (Vic-Snap, Correlated Solutions). The area of interest of the picture is masked into a region consisting of the whole surface of the samples, avoiding the edges near the grips. The masked area was divided into sub-images, or subsets, of 15 x 15 pixels with an overlap of 2 pixels. The distribution of the grey values in a subset of the picture, taken in the un-deformed state, corresponds to the distribution of the grey values of the same subset in the deformed state. By tracking the subsets in each successive image, relative displacements were obtained and the resulting strains were derived according to the digital image correlation algorithm.

Scanning electron microscopy (SEM) and energy dispersive x-ray analysis (SEM-EDX)

The morphology of the cross-sections of wood veneers, both laser-cut and tension-fractured, was observed using a field-emission scanning electron microscope (SEM) (Hitachi S-4800, Japan). Prior to examination, the cross-sections were sputter-coated with gold-palladium to a thickness of roughly 0.25 nm. The cross-section of the veneers was also analyzed using a JEOL JSM-6400 SEM coupled with energy dispersive X-ray analysis (EDX). Elemental measurements were performed at pinpoint areas of the sample 250 nm in diameter.

Dynamic mechanical analysis (DMA)

Temperature-dependent viscoelastic measurements were performed with a Perkin Elmer (Upplands Väsby, SE) DMA 7e instrument. The apparatus operated in a three-point bending mode with a span of 5 mm. Specimens were cut to rectangles of dimensions 2 mm (width) x 20 mm (length) along the wood fibers with a thickness of approximately 0.6 mm. They were impregnated with ethylene glycol at room temperature in a vacuum chamber and tested while immersed in ethylene glycol from 25 °C to 135 °C at a rate of 0.5 °C/min, with oscillation at a frequency of 0.6 Hz. The bending deformation amplitude was kept at 10 μ m. The softening temperature of wood was calculated as the maximum value of $\tan \delta$.

Resistivity measurements and calculation of conductivity

Treated and untreated veneers conditioned at 66% RH and 22 °C were cut to dimensions of 20 mm x 20 mm x 0.6 mm for conductivity measurements performed through the thickness of the veneers. For surface conductivity measurements, specimens of dimensions 0.6 mm x 5 mm x 25 mm were used.

A four-point probe with four gold wires in parallel was used to measure the conductivity in the plane of the veneers, both parallel to and normal to the fiber direction. Once the wires were placed in contact with the sample surface, a constant current was applied between the outermost wires (the working electrode (WE) and the counter electrode (CE)). The potential drop was measured between the innermost wires, (the reference electrodes (RE)), as shown in Fig. 2.

A Swagelok cell with a two-probe setup was used to measure the conductivity through the veneers. A sample was placed between two stainless steel plates and compressed until a constant reading was recorded. Constant current was applied through the sample while the potential was recorded.

To isolate the polymer effect, a reference sample was prepared. This sample was a non-treated veneer coated on both surfaces with an 8 wt.% aqueous PANI solution mixed at 0 °C to decrease the contact resistance between sample and the probe electrodes. The surface-coated sample was first impregnated with a water/phosphoric acid solution at a pH of 2 to saturate the structure, preventing penetration of the PA coating beyond the surface of the sample.

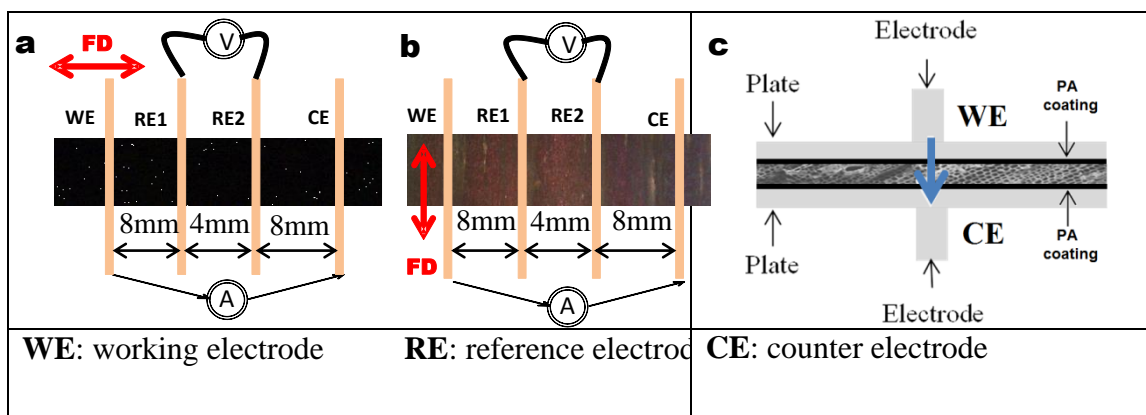


Fig. 2. a. Setup of surface electrical conductivity measurements using gold wires, along the fiber direction (FD); b. surface conductivity measurement across the fiber direction; and c. setup of conductivity measurements through the cross-section of wood veneers using a Swagelok cell

Resistance imaging

An Oltronix (Leek, NL) Power supply was used to provide 70 V to the electrodes clipped to the sample edges. One electrode was clipped on each end of the earlywood annual ring to generate current in the fiber direction. To generate current normal to the fiber direction, the electrodes were clipped parallel to each other on opposite edges of the veneer and were separated by approximately four annual rings. A FLIR I50 thermal imaging camera was used to generate images.

RESULTS AND DISCUSSION

Semiconductive wood was prepared by *in-situ* polymerization of conductive polyaniline in the structure of wood veneers. This method has been well-documented and was repeatable with and the weight percent gain (WPG) of polyaniline of 10 ± 1.5 wt. % to dry wood, measured by 5 separate samples (Treu *et al.* 2014). Phosphoric acid was chosen as the protic acid because this system has been well characterized and established in the literature and by the authors in previous work regarding polyaniline modified wood veneers (Trey *et al.* 2012). The morphology, conductivity, and mechanical properties of the modified veneers were characterized at different moisture contents. It was expected that the conductivity of the wood would increase with higher moisture contents and that the modified wood would have lower mechanical strength than the unmodified specimens. The morphology of the polymer in the wood structure and the characteristics of polyaniline-modified wood under a range of relative humidities are presented in this study.

PANI Modification in Relation to the Density and Moisture Content (MC)

Wood is a hygroscopic material in which the absorption of humidity from the surrounding environment depends on the amount of water within the wood, the relative humidity of the air, and the temperature of the air. The fiber saturation point (FSP) is the moisture content at which the cell walls are completely saturated with bound water. However, moisture is absent from the hollow center of the cell. Regardless of the wood species, the moisture content of wood is about 30%. The mechanical strength of wood increases as the MC drops below the FSP, with the exception of wood dried below 6% moisture (Gerhards 1980; Kretschmann and Green 1995).

To observe the effect of PA on the moisture uptake of wood veneers, the density and MC were determined for the EW and LW components of the untreated and treated veneers. When characterizing wood, the density of earlywood can vary greatly in comparison to that of latewood. These components of the veneers (both unmodified and modified) were measured separately for each of the three sets of environmental conditions chosen for this study (Table 1). A range of three humidities (0, 66, and 98% RH) was chosen to determine the effects of humidity on the mechanical properties and the moisture uptake of the modified veneers.

It was observed that the density did not vary to a large extent in normal (non-treated) veneers than in impregnated (treated) veneers. The density of EW was slightly higher in the treated samples, which is likely due to the deposition of a higher content of polyaniline particles in the lumen, as observed in the SEM-EDX results presented later in this study. There was a slight decrease in the density of LW with treatment, which may be due to a higher volume of hemicellulose being lost during the aniline treatment from areas containing more substantial cell wall structures as compared to EW.

It was not possible to determine the exact reason for the weight loss of the samples after treatment, as it was due to both the loss of wood extractives during the leaching process and the weight gain of PANI as a result of the impregnation process. For both the LW and EW specimens, the MC naturally increased with the RH at a similar ratio for both untreated and treated specimens. This demonstrates that the polyaniline treatment did not significantly affect the moisture sensitivity of the wood samples. Further, the density of the samples was not significantly affected by the polyaniline treatment.

Table 1. Densities and Moisture Contents of Wood Veneers with and without PANI at Different Relative Humidities

	Non-Treated						Treated					
	0% RH		66% RH		98% RH		0% RH		66% RH		98% RH	
	LW	EW	LW	EW	LW	EW	LW	EW	LW	EW	LW	EW
Density (g/cm³)	0.65	0.31	0.64	0.34	0.64	0.34	0.61	0.43	0.58	0.47	0.58	0.34
MC (%)	2.31	1.59	10.70	9.85	19.88	19.00	2.76	2.46	10.80	11.11	21.28	20.65

Effect of PANI Treatment on the Final Morphology of the Modified Wood Structure

To investigate the morphology of the polyaniline particles in the wood structure and to determine if the particles affected the failure pattern, cross-sections of the unmodified and PANI-modified veneers were imaged by SEM (Fig. 3). Cross-sections of veneers which had undergone tensile failure were prepared such that the interfaces between the wood structural regions and the polyaniline layer were more apparent. The fringes present in Fig. 3a are fiber bundles that were torn apart, resulting in dislocations that swept across the entire section as the stress increased, ultimately leading to tensile failure.

It is clear that the honeycomb structure of the wood was, in general, not changed by the treatment (Figs. 3a and 3c). However, the differences in the cell wall surfaces of the lumen are interesting. The untreated veneers had very smooth and even surfaces in the lumen (Figs. 3a and 3b) while the treated ones had rough, coarse surfaces (Figs. 3c and 3d). The PANI was attached to the cell walls in a distinct coating layer (Fig. 3d) roughly 0.3 μm in thickness. Figure 3d is an image of the cell wall of a specimen broken by tension, in which the thickness of the PANI layer is evident and is highlighted with arrows. The break pattern of the wood remained unchanged with the addition of polyaniline, indicating that the basic properties and structure of the wood remained intact following treatment.

No visible differences in the middle lamella of untreated and treated specimens were observed.

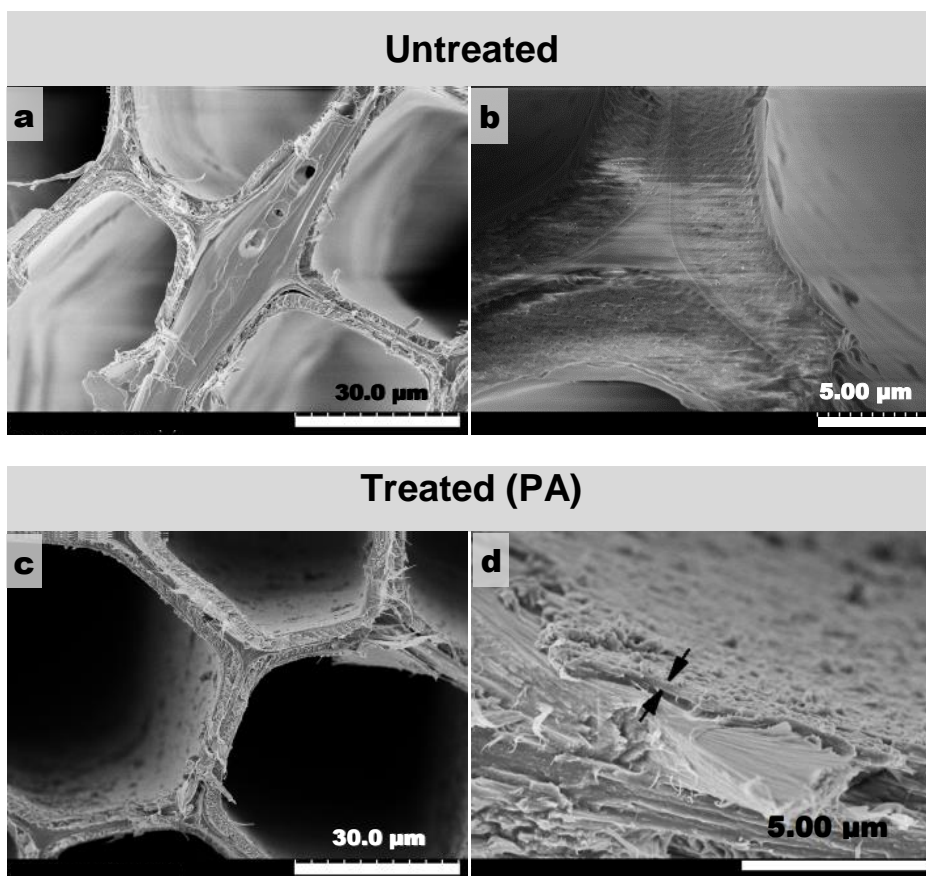


Fig. 3. (a) EW cell walls dislocated by tensile stress along the fiber direction; (b) image of a laser-cut EW cell wall focused on the middle lamella; (c) image of a treated LW cell; and (d) magnified area in which a layer of polyaniline, of about 0.3 μm thickness, is shown by the arrows

The SEM-EDX was used to quantify the PANI particles in the different structural sections of wood. Using this method, three different points were chosen on the wood cross-section: point 1 focused on the lumen wall; point 2, the middle lamella; and point 3, the cell wall (Fig. 4a). It should be mentioned that similar results were observed in duplicate samples and in other areas of the sample, but to simplify the illustration, only 3 points per sample are shown. In Figs. 4a and 4b, the backscattering electron image shows significant contrast between the elemental analyses (presented in Table 2). According to elemental analysis, the treated samples contained not only carbon and oxygen, but also nitrogen from the polyaniline, which was not detected in the untreated samples. The nitrogen content from polyaniline was found to be twice as high in the middle lamella as in the other structural parts of the wood (the cell wall and the lumen wall). The polyaniline deposited on the lumen wall is likely very porous, are separate particles, and does not thoroughly cover the lumen wall. It is unclear if this greater deposition of polyaniline in the middle lamella was a result of the greater porosity in the middle lamella allowing for more deposition of particles or if it was because lignin has a similar chemical structure to the aniline monomer, drawing more of the monomer to this area during polymerization. In placing wood samples in the aqueous polyaniline solution, we have observed swelling of the wood, indicating that the cell walls swell with the monomer solution. This would indicate no difficulty in the aniline monomer solution penetrating all areas of the wood and depositing in all regions of the wood structure.

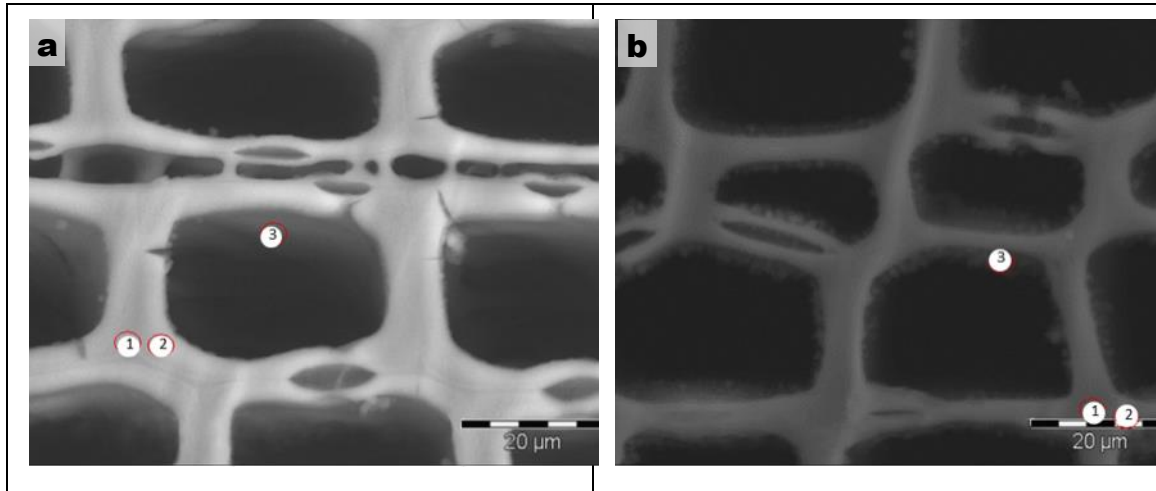


Fig. 4. (a) Image of untreated wood cross-section and (b) Image of treated wood generated by electron backscattering

Table 2. Summary of Elemental Analysis of Unmodified and Modified Wood

Untreated cross-section	Carbon wt. % (un/modified)	Oxygen wt. % (un/modified)	Nitrogen wt. % (un/modified)
Middle lamella (point 1)	65/64	35/28	Not detected/6
Cell wall (point 2)	67/58	33/36	Not detected/3
Lumen wall (point 3)	59/55	40/39	Not detected/3

Effect of PANI Modification on the Mechanical Strength of the Veneers

To determine how the addition of polyaniline affected the mechanical strength of the veneers, tensile testing was performed.

As stated previously, the physical and mechanical properties of wood do not increase with addition of water beyond the FSP. The FSP is about 30% and is unrelated to the wood species. The ultimate tensile strength parallel-to-grain first increases as the MC drops from 30 to 15% and then begins to decrease when the MC decreases below 10 to 15% (Green and Kretschmann 1994). The results displayed in Fig. 5 are consistent with that trend. The mechanical properties tended to decrease as the MC fell below 10% (corresponding to a RH of 66%, as shown in Table 1). A decrease in properties was observed in the specimens conditioned in environments above 66% RH. This was expected because the MC of the specimens was well above 10% when they were conditioned in an environment above 66% RH.

There was a notable decrease in the mechanical properties of the wood veneers after they were impregnated with PANI. Comparing EW and LW, the LW samples were stiffer and stronger, with the lowest strain at failure. A close look at the treated and non-treated results for EW and LW reveals a similar tendency. This behavior is logical and agrees with that of untreated wood, which is a clear indication that the PA affects the structure of the wood without changing its general morphology (as described in the previous section).

The difference between the average mechanical property values of treated and untreated samples became larger as the MC increased. This indicates a relationship between the PANI and the MC. Although the stiffness and strength declined after PANI modification, this reduction was not very large. Moreover, the failure mode remained the same in the PANI-modified specimens (

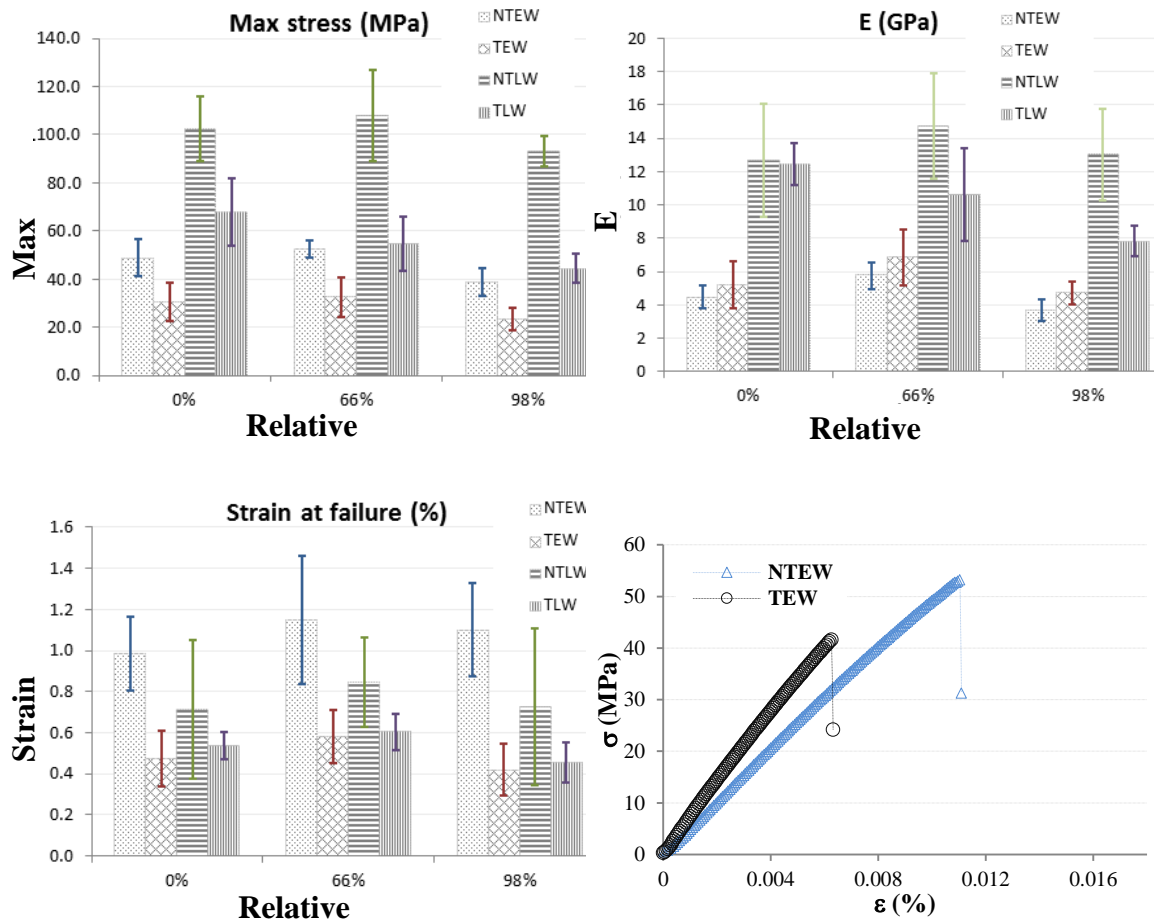


Fig. 5. (a) 5d); the specimens failed *via* brittle fracture.

Wood is a complex structure consisting of discontinuous fibers that are primarily composed of cellulose embedded in an organic lignin matrix. The intricate structure of wood is, among other things, generated by the interconnectivity of anatomical structures called pits. The pits allow different levels of fluid mobility, as these structures are normally matched in pairs between adjacent cells. This facilitates PANI impregnation. However, due to their small size, pits can easily become clogged. From a mechanical point of view, it has been suggested that the pits can be a source of stress due to the irregularities in the fiber structure (Sirvio and Karenlampi 1998). Pits clogged with PANI can be one of the reasons for the decrease in mechanical properties observed after treatment. Most important is the loss of degraded hemicellulose components, which has been found to cause 1 to 2 wt. % mass loss. This was shown to be a result of the low pH of 2 during the polyaniline polymerization process. Such weight loss (due to an impregnation process) has previously been reported to result in decreased mechanical properties (Sundkvist *et al.* 2006).

The effects of PANI on EW are different than they are on LW. In latewood, it can be said that in general, from Figs. 5a to 5c, that the Young's modulus decreased with the addition of polyaniline. It has been reported that there is more lignin content and less cellulose in LW as compared to EW (Bertaud and Holmbom 2004). Because polyaniline

appears to be most concentrated in the middle lamella (as observed by SEM-EDX), this corresponds to the larger effect of polyaniline on the modulus in the LW. This is also true at 0% RH; with the addition of water, the sample was softened and the modulus decreased. This could be due to the thicker cell walls of latewood. In earlywood, the addition of PANI had less of an effect on the modulus and maximum stress. However, the strain at failure decreased. This was likely a result of the loss of hemicellulose affecting the thin walls of EW to a larger degree than those of the lignin-rich LW.

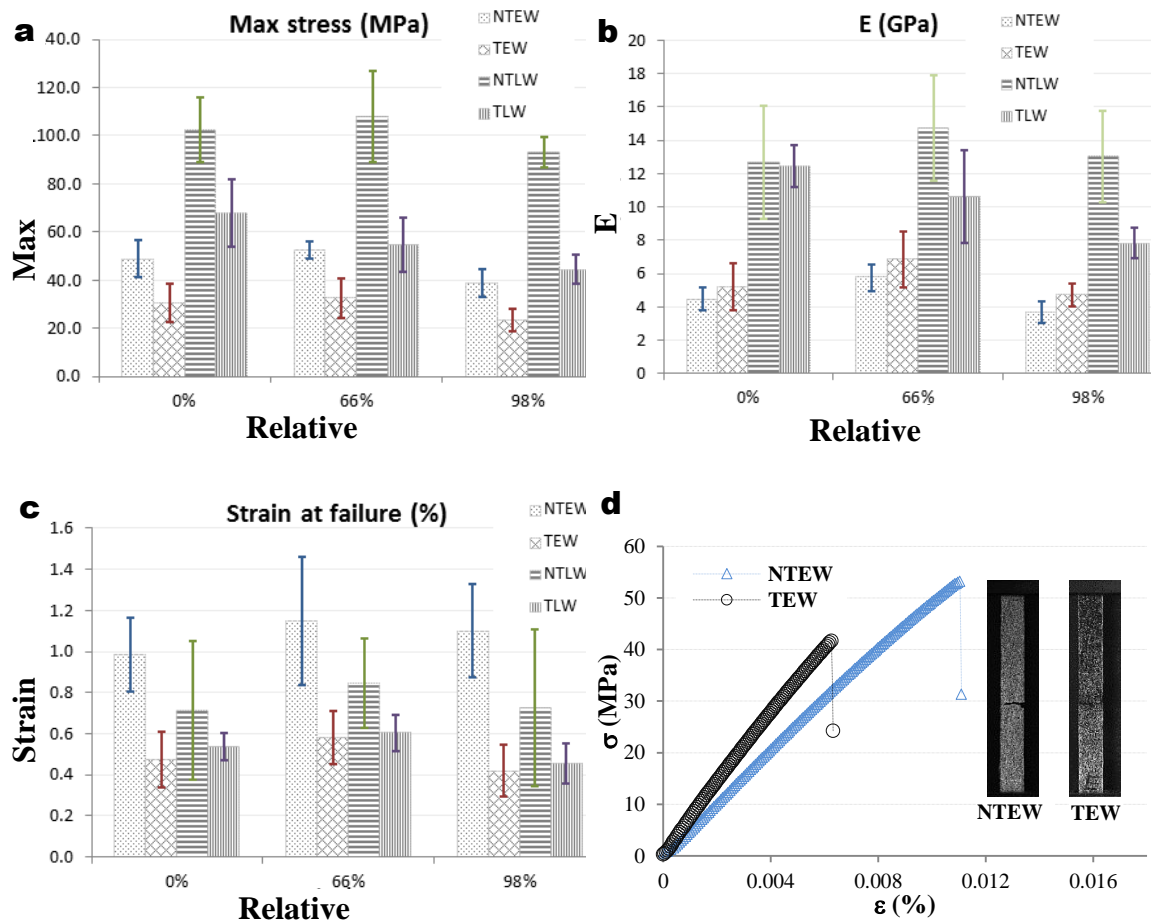


Fig. 5. (a) Young's modulus of treated and untreated wood veneers for different moisture contents; (b) Values of tensile maximum stress in terms of MC; (c) Strain at failure of wood veneer specimens tested under tension; and (d) Stress-strain curves and photographs of untreated and treated tensile specimens at the moment of failure. Abbreviations used in this figure include: treated earlywood (TEW), non-treated earlywood (NTEW), treated latewood (TLW), and non-treated latewood (NTLW)

Effects of Interactions between Polyaniline and Lignin in the Wood Veneers

Because there is a high content of lignin in the middle lamella, and PANI was observed to be in higher concentrations in this region by SEM-EDX, it is of interest to look more closely at the interactions between lignin and polyaniline. The lignin thermal transition can be observed by DMA when the lignin has been softened with ethylene glycol, which plasticizes southern yellow pine veneers similarly to water (Bouajila *et al.* 2006; Salmén *et al.* 1996). In this study, the softening temperature, or glass transition temperature

(T_g), of the untreated and treated veneers was determined from the peak of the $\tan \delta$ curve (Fig. 6). Considering the natural heterogeneity of wood and that T_g is reported to vary widely (by approximately 40 °C), suitable reproducibility for each specimen type was observed for the T_g values determined, with a reproducible curve shape and peak broadness (Cronier *et al.* 2005; Salmén 1984) (Fig. 6).

The addition of PANI to the structure of the wood veneers slightly lowered the T_g of wet lignin (Fig. 6). In the case of EW, the T_g shifted from 99 to 96 °C, whereas in LW, the T_g decreased from 95 to 89 °C. The greater shift in the lignin T_g of LW, compared to that of EW, further indicates that the higher lignin content of LW caused the T_g of lignin to decrease more dramatically. These results indicate that the polyaniline present in the wood structure does interact to a significant degree with lignin. It is possible that the polyaniline particles break up the compact structure of lignin, providing more voids and overall volume in the structure. The loss of hemicelluloses, with the low pH polyaniline deposition process, could also contribute to the lower transition of lignin by contributing to separation of the polymer chains and the resulting voids creating less internal friction. It is also possible that the addition of PANI inhibited the secondary interactions of the wood structure components. This result correlates to the mechanical properties, in that E , σ_{max} , and ϵ_{max} decreased with rising moisture content and that this reduction of mechanical properties was more significant in latewood samples. The larger the amount of polyaniline attached to the cell wall, the more rigid and moisture-sensitive the wood became.

By observing the differences in the strain at failure, the degradation effect of the addition of PANI on earlywood becomes evident (Fig. 5).

During measurement by DMA, the gauge length was reduced in order to prevent the samples' resonant frequencies from disrupting the results. However, this resulted in storage modulus values that were unreliable for stiffness considerations. Therefore, the storage modulus is not presented.

Because the $\tan \delta$ describes a material's damping characteristics and is defined as the energy ratio between the loss and storage moduli, a high $\tan \delta$ indicates energy loss due to molecular rearrangement and internal friction (Turi 1997). In both the EW and LW treated samples, there was a reduction in the $\tan \delta$ curve, signifying less internal friction and a separation of the polymer chains from one another (Fig. 6). This further confirms that the polyaniline particles break up the secondary interactions between the polymer chains of the wood components.

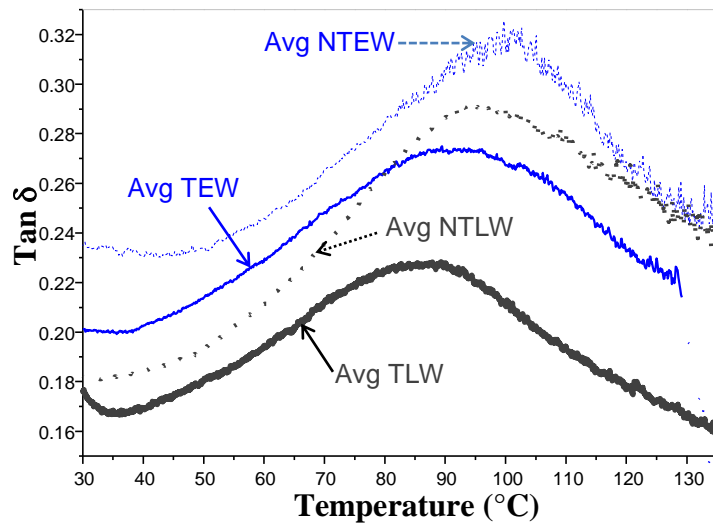


Fig. 6. Average $\tan \delta$ curves for each group of test specimens; treated earlywood (TEW), non-treated earlywood (NTEW), treated latewood (TLW), and non-treated latewood (NTLW)

Conductivity as a Function of Fiber Direction

Conductivity measurements were made to analyze the effect the anisotropic structure of wood on the pathway of current through PA-modified wood.

The impregnation process resulted in wood veneers with high electrical conductivity. Untreated veneers had a surface conductivity of 3.0×10^{-7} S/m across and along the fibers, whereas PA-impregnated wood had higher conductivities of 4.0×10^{-4} S/m across the fibers and 4.0×10^{-3} S/m along the fiber direction (Table 2). The one-decade difference between the values across and along the fiber direction reveals the anisotropic behavior of the treated veneers, in terms of their electrical conductivity. These results indicate that a path of higher conductivity, provided by a more complete physical network of connecting conductive polyaniline particles, was through the PA in the cell walls that were oriented in the fiber direction. The wood structure is complex and this data indicates that along the fiber direction, the structure of the wood aides a network of connecting particles, perhaps by orienting the particles along the cell walls or lumen. The direction normal to the fiber has lower conductivity indicating that the wood structure hinders the physical connectivity of the polyaniline particle network in this direction. This may be a result of voids or polyaniline-deficient regions that inhibit the percolation of electrical conductivity.

Measurements were taken through the cross-section of the untreated, superficially coated, and treated wood samples in order to find the electrically conductive pathways through the wood structures. For untreated wood at 66% RH and 20 °C, the measurements through the thickness of the veneers were near the lower boundary of the potentiostat capabilities, with conductivity lower than 1.0×10^{-15} S/m. The control sample showed almost no difference, with a conductivity of less than 1.0×10^{-13} S/m. However, values for the veneers impregnated with PANI increased to 6.8×10^{-6} S/m. Considering the cross-sectional measured values of samples with and without treatment (Table 2) and the honeycomb structure of wood, it is apparent that high conductivity is possible only when PA has penetrated the cell walls. Electric current follows a path along the length of the cell walls. Although a higher density of PANI was observed in the middle lamella compared to the cell wall, the conductivity did not appear to increase normal to the fiber direction. One

explanation for this could be that voids between the cell walls and the middle lamella created regions of electrical discontinuity.

Table 3. Electrical Conductivities Measured on the Surfaces and Through the Cross-sections of Wood Veneers

	Surface conductivity (S/m)		Conductivity through cross-section (S/m)
	Along the fibers	Across the fibers	
Non-treated	3.0×10^{-7}	3.0×10^{-7}	$< 1.0 \times 10^{-15}$
Surface coated	-	-	$< 1.0 \times 10^{-13}$
Treated	4.0×10^{-3}	4.0×10^{-4}	6.8×10^{-6}

To visually observe the pathway of current through the untreated and treated wood, a power source with electrodes was used to send a current through the materials and the samples were imaged with a thermal camera. The sample positioning is shown in Fig. 7a, in which the electrodes were clipped to the edges of the wood veneers. The thermal images displayed a temperature of 21.7 °C in the untreated specimen, as shown in Fig. 7b. There was no detection of added heat in the sample with the addition of current in the fiber direction (Fig. 7c). The treated sample without applied current is shown in Fig. 7d. With the addition of current, a thermal band appeared along the fiber direction, within the annual ring pattern. This shows the path of the current. The significant increase in temperature demonstrates that the majority of the current passed through this pathway. This was strongest at the source (at 37.8 °C) and was almost undetectable in the neighboring annual ring (at 22.4 °C) (Fig. 7e). When current was applied normal to the fiber direction, the temperature increase was only minute, with a peak temperature of 25.3 °C (Fig. 7f). These results confirmed that the resistance in the material was anisotropic. The resistance was lower in the direction along the fibers than in the direction against the fiber, so the current was concentrated in a single pathway when the voltage was applied along the fibers and was diffused across the entire sample when it was applied against the fibers.

This not only shows the pathway of conductivity through the veneer, but also illustrates that wood modified with polyaniline could be used for certain types of heating applications.

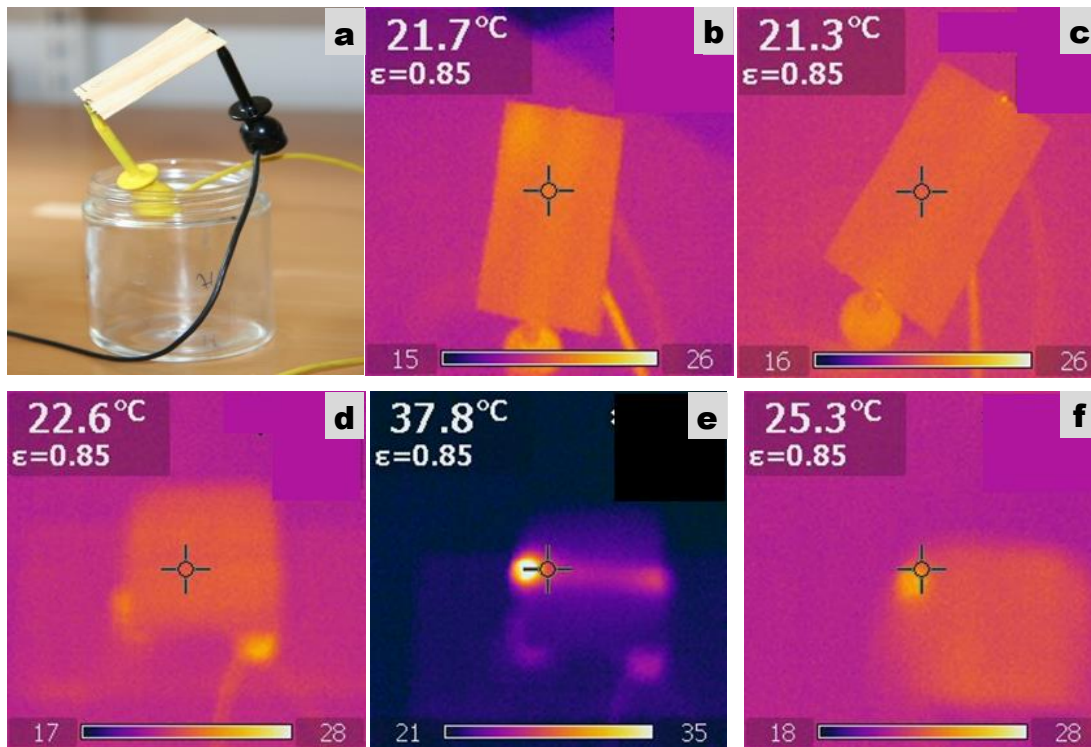


Fig. 7. (a) image of a veneer with a CRL camera; (b) thermal image of an untreated veneer without applied current; (c) thermal image of an untreated veneer with applied current; (d) thermal image of a treated veneer with no applied current; (e) thermal image of a treated veneer with applied current in the fiber direction; and (f) treated sample with current applied normal to the fiber direction

CONCLUSIONS

1. It was found that the entire structure of wood is affected by PANI impregnation.
2. The PANI adhered to the lumen and cell walls and formed more significantly in the cell walls and middle lamella, as confirmed by SEM-EDX. Despite this, no significant difference was observed in the ratio of equilibrium moisture uptake between untreated and treated samples with increasing relative humidity.
3. The PANI modification resulted in a reduction of the storage modulus, the maximum strength, and the ductility of the wood, possibly because PANI particles interfered with the natural, strength-providing secondary interactions within the cell wall.
4. With the addition of PANI, the wood veneers became anisotropic semiconductors, in which the current travelled most easily along the direction of the wood fibers. This indicates that the template of the wood, infused with particles in the wood cell walls and middle lamella, allows for the directional control of the resulting semiconducting properties.
5. A strong interaction was observed between PANI and the lignin component of the wood veneers, as confirmed by the decrease in the lignin glass transition temperature (T_g) with the addition of PANI. However, the complex structure of the wood remained intact despite a large loading of PANI particles. This could allow for a lightweight, wood-

based semiconducting material to complement current plastic matrix composite materials.

ACKNOWLEDGEMENTS

The Wallenberg Wood Science Center (WWSC) and the KTH Royal Institute of Technology are thanked for their funding. Ann-Mari Olsson and Lennart Salmén are thanked for their help and knowledge regarding DMA and interpretation of its results. Rodrigo Robinson of SP CMY is thanked for his assistance with SEM-EDX. Joachim Seltman is thanked for his sample preparation with the excimer laser.

REFERENCES CITED

- Ansari, R. (2006). "Application of polyaniline and its composites for adsorption/recovery of chromium (VI) from aqueous solutions," *Acta Chim. Slov.* 53(1), 88-94.
- Bertaud, F., and Holmbom, B. (2004). "Chemical composition of earlywood and latewood in Norway spruce heartwood, sapwood and transition zone wood," *Wood Sci. Technol.* 38(4), 245-256.
- Bouajila, J., Dole, P., Joly, C., and Limare, A. (2006). "Some laws of a lignin plasticization," *J. Appl. Polym. Sci.* 102(2), 1445-1451.
- Cronier, D., Monties, B., and Chabbert, B. (2005). "Structure and chemical composition of bast fibers isolated from developing hemp stem," *J. Agric. Food Chem.* 53(21), 8279-8289.
- Gerhards, C. C. (1980). "Effect of moisture content and temperature on the mechanical properties of wood: An analysis of immediate effects," *Forest Products Laboratory, Forest Service, U.S. Department of Agriculture, Madison, WI.*
- Green, D. W., and Kretschmann, D. E. (1994). "Moisture content and properties of clear southern pine," *US Department of Agriculture, Forest Service, Forest Products Laboratory, Madison, WI.*
- Heeger, A. J. (2001). "Semiconducting and metallic polymers: The fourth generation of polymeric materials," *J. Phys. Chem. B* 105(36), 8475-8491.
- Huang, W. S., Humphrey, B. D., and MacDiarmid, A. G. (1986). "Polyaniline, a novel conducting polymer - Morphology and chemistry of its oxidation and reduction in aqueous-electrolytes," *J. Chem. Soc. Farad. T.* 1 82(1), 2385-2400.
- Jafarzadeh, S., Johansson, M., Sundell, P.-E., Claudino, M., Pan, J., and Claesson, P. M. (2013). "UV-curable acrylate-based nanocomposites: Effect of polyaniline additives on the curing performance," *Polym. Adv. Tech.* 24(7), 668-678.
- Kretschmann, D. E., and Green, D. W. (1995). "Modeling moisture content - Mechanical property relationships for clear Southern Pine," *USDA, Forest Service, Forest Products Laboratory, Madison, WI.*
- Madani, M., Aly, S. S., and El-Sayed, S. M. (2010). "Dielectric relaxation of new aniline methyl methacrylate copolymer synthesized by gamma irradiation initiated polymerization," *High Perform. Polym.* 22(5), 515-533.
- Park, S. K., Lee, S. Y., Lee, C. S., Kim, H. M., Joo, J., Beag, Y. W., and Koh, S. K. (2004). "High energy (MeV) ion-irradiated π -conjugated polyaniline: Transition from insulating state to carbonized conducting state," *J. Appl. Phys.* 96(4), 1914-1918.

- Qaiser, A. A., Hyland, M. M., and Patterson, D. A. (2009). "Control of polyaniline deposition on microporous cellulose ester membranes by in situ chemical polymerization," *J. Phys. Chem. B* 113(45), 14986-14993.
- Razak, S. I. A., Rahman, W. A. W. A., Sharif, N. F. A., Nayan, N. H. M., Saidi, M. A. A., and Yahya, M. Y. (2013). "Polyaniline coated kenaf core and its effect on the mechanical and electrical properties of epoxy resin," *Composite Interfaces* 20(8), 611-622.
- Rimbu, G. A., Stamatini, I., Jackson, C. L., and Scott, K. (2006). "The morphology control of polyaniline as conducting polymer in fuel cell technology," *J. Optoelectron. Adv. Mater.* 8(2), 670-674.
- Saini, P., and Arora, M. (2013). "Formation mechanism, electronic properties & microwave shielding by nano-structured polyanilines prepared by template free route using surfactant dopants" *J. Mater. Chem. A* 1, 8926-8934.
- Salmén, L. (1994). "Viscoelastic properties of in situ lignin under water-saturated conditions," *J. Mater. Sci.* 19(9), 3090-3096.
- Salmén, L., Olsson, A. M., and Wennerblom, M. (1996). "The effect of lignin composition on the viscoelasticity properties of wood," *Nord. Pulp Pap. Res. J.* 4(1), 279-280.
- Sirvio, J., and Karenlampi, P. (1998). "Pits as natural irregularities in softwood fibers," *Wood Fiber Sci.* 30(1), 27-39.
- Treu, A., Bardage, S., Johansson, M., and Trey, S. (2014). "Fungal durability of polyaniline modified wood and the impact of a low pulsed electric field," *Int. Biodeter. Biodegr.* 87, 26-33.
- Trey, S., Jafarzadeh, S., and Johansson, M. (2012). "In situ polymerization of polyaniline in wood veneers," *ACS Appl. Mater. Interfaces* 4(3), 1760-1769.
- Turi, E. A. (1997). *Thermal Characterization of Polymeric Materials*, 2nd Ed., Vol. 1, Academic Press, Brooklyn, NY.
- Wang, J., Zhang, and K. Zhao, L. (2014). "Sono-assisted synthesis of nanostructured polyaniline for adsorption of aqueous Cr(VI): Effect of protonic acids," *Chem. Eng. J.* 239, 123-131.
- Wolszczak, M., Kroh, J., and Abdel-Hamid, M. M. (1995). "Some aspects of the radiation processing of conducting polymers," *Radiat. Phys. Chem.* 45(1), 71-78.

Article submitted: February 24, 2014; Peer review completed: May 7, 2014; Revised version accepted: May 19, 2014; Published: July 9, 2014.